



An improved atmospheric weighted mean temperature model and its impact on GNSS precipitable water vapor estimates for China

Liangke Huang^{1,2} · Lilong Liu^{2,3} · Hua Chen⁴ · Weiping Jiang¹

Received: 29 August 2018 / Accepted: 11 March 2019 / Published online: 18 March 2019
© Springer-Verlag GmbH Germany, part of Springer Nature 2019

Abstract

The atmospheric weighted mean temperature, T_m , is an important parameter for retrieving precipitable water vapor (PWV) from global navigation satellite system (GNSS) signals. There are few empirical, high-precision T_m models for China, which limit the real-time and high-precision application of GNSS meteorology over China. The GPT2w (Global Pressure and Temperature 2 Wet) model, as a state-of-the-art global empirical tropospheric delay model, can provide values for T_m , surface temperature, surface pressure, and water vapor pressure. However, several studies have noted that the GPT2w model has significant systematic errors in the calculation of T_m for China, mainly due to the neglect of the T_m lapse rate. We develop an improved T_m model for China, IGPT2w, by refining the T_m derived from GPT2w using both gridded T_m data and ellipsoidal height grid data from the Global Geodetic Observing System (GGOS) Atmosphere. Both gridded T_m data from the GGOS Atmosphere and radiosonde data from 2015 are used to test the performance of IGPT2w in China. The results are compared with the GPT2w model and the widely used Bevis formula. The results show that IGPT2w yields significant performance against other models in T_m estimation over China, especially in western China, where the significant systematic errors of the GPT2w model are largely eradicated. IGPT2w has σ_{PWV} and σ_{PWV}/PWV values of 0.29 mm and 1.38% when used to retrieve GNSS-PWV, respectively. Thus, the IGPT2w has significant potential for real-time GNSS-PWV sounding in China, especially when used to retrieve GNSS-PWV values for the study of PWV transportation in the Tibetan Plateau.

Keywords Weighted mean temperature · GGOS Atmosphere · GPT2w model · Precipitable water vapor

Introduction

Water vapor, an important part of the atmospheric system, has attracted great attention in the study of weather and long-term climate, such as in research on global water cycling and energy balances (Wang et al. 2007; Wang and Zhang 2009; Jin and Luo 2009). Traditional water vapor monitoring techniques mainly depend on radiosondes, satellite-based instruments, and water vapor radiometers. Such

conventional techniques have limitations in capturing fine variations due to their low spatiotemporal resolutions. The drawbacks of these traditional techniques are increasingly clear with the growing demands of modern meteorological applications. To overcome the shortages of these techniques, a global positioning system (GPS) technique is extensively being used to compensate for these disadvantages. Bevis et al. (1992) first proposed the use of GPS measurements to sense precipitable water vapor (PWV). Great efforts have been conducted to sense PWV using GPS/GNSS measurements (Rocken et al. 1995; Li et al. 2015; Manandhar et al. 2017). There has been a rapid establishment of GNSS monitoring stations network at the regional, national and global scales. The PWV data retrieved from GNSS signal are widely used for the analysis of severe weather conditions, such as heavy rainfall (Adams et al. 2013; Zhang et al. 2015; Benevide et al. 2015), flood (Suparta and Rahman 2016; Huelsing et al. 2017), drought (Jiang et al. 2017) and typhoon events monitoring (Zhao et al. 2018).

✉ Weiping Jiang
wpjiang@whu.edu.cn

¹ GNSS Research Center, Wuhan University, Wuhan 430079, China

² College of Geomatics and Geoinformation, Guilin University of Technology, Guilin 541004, China

³ Guangxi Key Laboratory of Spatial Information and Geomatics, Guilin 541004, China

⁴ School of Geodesy and Geomatics, Wuhan University, Wuhan 430079, China

Electromagnetic signals sent by a GNSS satellite through the neutral atmosphere are affected by troposphere refraction, resulting in a tropospheric delay. This delay along the zenith path is defined as zenith total delay (ZTD). The ZTD can be divided into two components, i.e., zenith hydrostatic delay (ZHD) and zenith wet delay (ZWD). Bevis et al. (1992) proposed an approach to derive the atmospheric weighted mean temperature (T_m) for deriving PWV from the ZWD of GNSS signals. The ZTD can be precisely estimated from GNSS observations using a precise point positioning (PPP) technique or differential approaches. The ZHD can also be accurately calculated from an empirical tropospheric delay model, and the ZWD can be calculated by subtracting ZHD from ZTD. Therefore, once the ZWD is calculated, the PWV value can be estimated. The role of T_m in the process of PWV estimation is as follows (Davis et al. 1985; Askne and Nordius 1987; Bevis et al. 1994; Ross and Rosenfeld 1997):

$$PWV = \Pi \cdot ZWD \tag{1}$$

$$\Pi = \frac{10^6}{\rho_w R_v \left(\frac{k_3}{T_m} + k'_2 \right)} \tag{2}$$

$$T_m = \frac{\int (e/T)dH}{\int (e/T^2)dH} \tag{3}$$

where Π is the dimensionless atmospheric conversion factor, ρ_w is the density of water, R_v is the specific gas constant for water vapor, k'_2 and k_3 are the atmospheric refractivity constants given in Bevis et al. (1994), e denotes the water vapor pressure (hPa) and T denotes the absolute temperature (Kelvin). The calculating precision of PWV depends on multiple error sources. According to the law of error propagation, the error of PWV can be deduced from (1) and (2), and the following formulas illustrate how the errors can affect PWV (Yao et al. 2014a),

$$\mu_{PWV} = \Pi \cdot \mu_{ZWD} + ZWD \cdot \mu_{\Pi} \tag{4}$$

$$\mu_{\Pi} = \frac{10^6 k_3}{\rho_w R_v (k_3 + k'_2 T_m)^2} \mu_{T_m} \tag{5}$$

where μ_{PWV} , μ_{T_m} , μ_{ZWD} , and μ_{Π} denote errors from PWV, T_m , ZWD, and Π , respectively. Currently, the International GNSS Service (IGS) provides the ZTD product with a precision of better than 5 mm (Byun and Bar-Sever 2009). The ZHD can be accurately estimated using numerical weather models or surface pressure observations (Hobiger et al. 2008a; Lu et al. 2016). In real-time, one can use a short-range forecast from a weather model to derive ZHD (Hobiger et al. 2008b; Lu et al. 2017). Thus, the ZWD can

be accurately obtained. Yao et al. (2014a) noted that the estimation error of PWV caused by ZWD error is approximately 1.5 mm if the ZWD has an estimation error of 1 cm. The accuracy of T_m , under this circumstance, is considered to have a dominant role in precise PWV calculation. In other words, precisely estimating T_m is the key to enhancing the precision of PWV estimation.

Multi-source atmospheric profiles, such as radiosonde profiles, the America National Centers for Prediction (NCEP) reanalysis data, and the European Center for Medium-Range Weather Forecasts (ECMWF) reanalysis data, can be used to calculate T_m . The T_m can be accurately estimated at a specific position using these atmospheric profiles based on the integration method. An accurate empirical model for T_m is needed to enhance the efficiency of T_m estimation and provide easy accessibility for users. Numerous studies have been conducted on T_m modeling, and a great number of empirical T_m models have also been developed for retrieving GNSS-PWV. Bevis et al. (1992) first introduced the concept of GPS meteorology and a widely used T_m model. The Bevis formula ($T_m = a + bT_s$), was developed by investigating the correlation between surface temperature (T_s) and T_m . The Bevis model has gained increasing attention and it has been found that the coefficients of a and b are largely depend on location and season and should be re-estimated using local observations for use in specific areas (Bevis et al. 1992; Ross and Rosenfeld 1997). Yao et al. (2014a) analyzed the relationship between T_m and surface meteorological parameters, such as T_s , P_s , and e_s , and then proposed a one-factor and a multi-factor T_m models that take geographic and seasonal variations into account. The two new empirical models obtained better results around the globe. Ding (2018) developed a new global T_m model, the NN model, based on the neural network algorithm, which only requires surface temperature as input. These empirical regression T_m models can obtain excellent results if in situ surface meteorological observations are available. Most GPS/GNSS monitoring stations, however, are initially installed for the purposes of geodesy, i.e., no meteorological instruments are installed at these GPS/GNSS stations. Therefore, these T_m models cannot be used for real-time retrieval of the GNSS-PWV due to the lack of in situ meteorological observations.

To obtain real-time retrieval of GNSS-PWV, Emardson and Derks (2000) proposed an empirical T_m model in Europe, which takes the seasonal and latitude variation of T_m into account and does not require in situ meteorological observations for the determination of real-time GNSS-PWV. In recent years, the non-meteorological parameter T_m models have received great attention as they are widely used for real-time GNSS meteorology. Yao et al. (2015) improved the T_m model developed by Emardson et al. and established a new empirical atmospheric conversion factor (Π) model for

low-latitude China. Yao et al. (2012) developed a global T_m model, the Global Weighted Mean Temperature (GWMT) model, using the spherical harmonics method. This new model can obtain excellent mean results over the globe; however, a relatively worse result was observed in parts of the southern Pacific Ocean due to the uneven distribution of the radiosonde stations involved in modeling. Yao et al. (2013) improved the GWMT model by combining the Bevis formula and the global pressure and temperature (GPT) model (Böhm et al. 2007), and an improved global T_m model, GTm-II, was proposed. Chen et al. (2014) established a new global empirical T_m model, GTm_N, using the NCEP reanalysis outputs, which considers both annual and semi-annual variations of T_m . Yao et al. (2014b) further refined previous models and then constructed a new global T_m model (GTm-III). He et al. (2017) developed a global T_m model (GWMT-D), which considers the height correction of T_m and yields remarkable performance over the globe. Furthermore, Huang et al. (2019) constructed a new global grid T_m model (GGTm) by employing the sliding window algorithm, which takes both latitude and altitude variation of T_m into account in modeling and performs excellent and reliable performance on a global scale.

Great efforts have been conducted towards developing global empirical T_m models. However, high-precision empirical T_m models for China are still lacking, which limits the real-time and high-precision application of GNSS meteorology for China. China is a vast territory that contains complex undulating terrain and diverse climate systems, especially in the Qinghai–Tibetan and Yunnan–Guizhou plateaus, where only a few radiosonde stations are available. Additionally, the GNSS-PWV sounding has not yet been fully conducted in China. In recent years, the Crustal Movement Observation Network of China (CMONOC), which contains over 260 GNSS monitoring stations, has been gradually applied in geodesy and geodynamics and can provide continuous long-term GNSS measurements for the potential application in PWV retrieval. Thus, there is an urgent need to develop a high-precision empirical T_m model for China for real-time GNSS-PWV retrieval.

The GPT2w (Global Pressure and Temperature 2 Wet) model developed by Böhm et al. (2015) is one of the newly released global tropospheric delay models and can also provide T_m . It should be noted that the GPT2w has excellent performance in T_m estimation compared to other existing empirical models. Several investigations have been conducted on the GPT2w model showing a systematic bias in T_m calculation (Zhang et al. 2017; Huang et al. 2019), mainly because the vertical correction of T_m is ignored. Generally, understanding the spatial–temporal characteristics of the T_m lapse rate is helpful in establishing a more sophisticated T_m model. However, the analysis of sophisticated seasonal characteristics of the T_m lapse rate is still lacking. In this

study, we investigate the spatial–temporal characteristics of the T_m lapse rate in China using both gridded T_m data and ellipsoidal height grid data from the Global Geodetic Observing System (GGOS) Atmosphere. An improved T_m model, namely, IGPT2w, will be developed by refining the T_m derived from GPT2w model for China. The performance of IGPT2w will be evaluated using gridded T_m data and radiosonde profiles.

Data description and T_m calculation

In this work, the gridded data derived of the GGOS Atmosphere are used to investigate the spatiotemporal characteristics of the T_m lapse rate and also to develop the IGPT2w model. Both gridded T_m data and radiosonde profiles are employed to validate the performance of new model.

Gridded data from GGOS Atmosphere

GGOS Atmosphere can provide continuous long-term global surface atmospheric grid products, such as T_m , ZHD, and ZWD, which are derived from ECMWF reanalysis data and all correspond to the ellipsoidal heights. These surface grid data have a temporal resolution of 6 h and a spatial resolution of $2.5^\circ \times 2^\circ$ (lon. \times lat) (<http://ggosatm.hg.tuwien.ac.at>). In addition, the global ellipsoidal height grid data, which have the same spatial resolution as the gridded T_m data, are also provided by the GGOS Atmosphere. Yao et al. (2014b) evaluated global surface gridded T_m data and showed that the gridded T_m data are highly accurate and reliable, which can be used to investigate spatial–temporal characteristics of T_m as well as for T_m modeling. In this study, we utilize gridded T_m data from 2007 to 2014 and ellipsoidal height grid data to investigate the T_m vertical features and the seasonal variations of T_m lapse rates and for T_m modeling in China. The gridded T_m data in 2015 are treated as reference values for validating the IGPT2w model.

Radiosonde profiles

The websites of the University of Wyoming freely provide global radiosonde observations (<http://weather.uwyo.edu/upperair/sounding.html>). Currently, there are in total more than 1500 radiosonde stations globally. The radiosonde profiles, with a resolution of 12 h, i.e., at UTC 00:00 and 12:00 every day, mainly include pressure level profiles and surface observations. In this study, a total of 89 radiosonde stations in China are selected (Fig. 1). The T_m values in 2015 derived from radiosonde observations based on the integration method are regarded as reference values to evaluate the IGPT2w for China. Additionally, the T_s data in 2015 obtained from radiosonde stations are used for the T_m

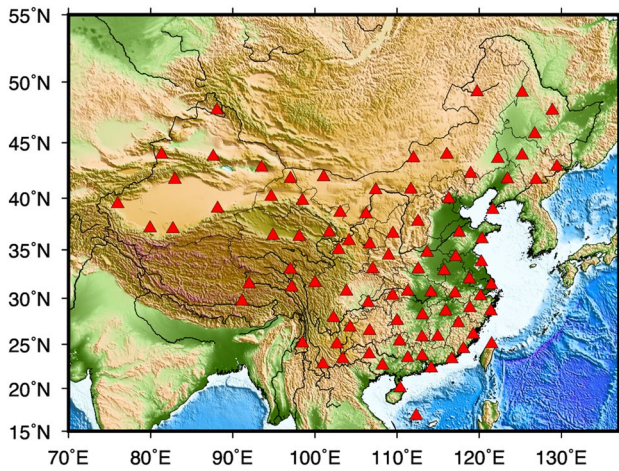


Fig. 1 Geographic and topographic distribution of the 89 radiosonde stations in China. The upward triangles denote the radiosonde stations

calculation in the Bevis formula ($T_m = 70.2 + 0.72T_s$) and the PWVs in 2015 received from radiosonde profiles are used to investigate the impact of T_m on GNSS-PWV. Here, for more convenient calculation, the integral formula (3) for calculating T_m can be discretized as follows:

$$T_m = \frac{\int (e/T)dH}{\int (e/T^2)dH} = \frac{\sum_1^n F_1(e_i, T_i)\Delta H_i}{\sum_1^n F_2(e_i, T_i)\Delta H_i} \quad (6)$$

where $F_1(e_i, T_i) = \frac{e_i}{T_i}$; $F_2(e_i, T_i) = \frac{e_i}{T_i^2}$; T_i and e_i are the average temperature and water vapor pressure at the i th layer of the atmosphere, respectively; ΔH_i denotes the thickness of the atmosphere at the i th layer (m), and n is the number of layers. As e cannot directly be obtained from radiosonde profiles, it can be calculated by the following formulas (Bolton 1980; Wang et al. 2016):

$$e = \frac{RH \cdot P_v}{100} \quad (7)$$

$$P_v = 6.11 \times 10^{\left(\frac{7.5 \times T_a}{237.3 + T_a}\right)} \quad (8)$$

where RH is the relative humidity, P_v and T_a are the saturated vapor pressure and the atmospheric temperature in celsius ($T = T_a + 273.15$) respectively.

Improving the T_m derived from GPT2w model in China

The GPT2w model can provide several meteorological parameters, such as T_m , T_s , P_s , e_s , and water vapor pressure lapse rate (λ), with two horizontal resolutions of $1^\circ \times 1^\circ$

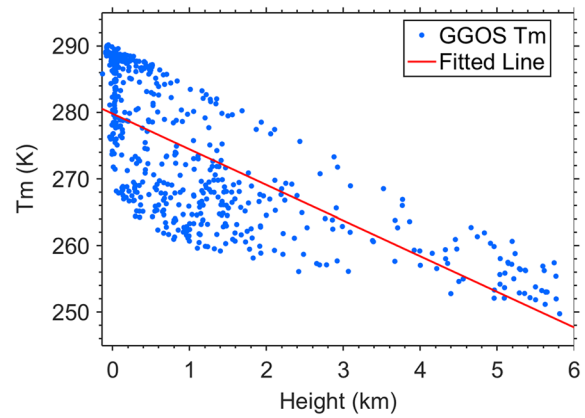


Fig. 2 T_m changes with height in China. The scatter points indicate the annual mean gridded T_m data in 2014 in China, and the red line indicates the linear fitted line for the vertical dependence of T_m

and $5^\circ \times 5^\circ$. The T_m can be estimated using the following formula:

$$T_m^r = \beta_0 + \beta_1 \cos\left(2\pi \frac{\text{doy}}{365.25}\right) + \beta_2 \sin\left(2\pi \frac{\text{doy}}{365.25}\right) + \beta_3 \cos\left(4\pi \frac{\text{doy}}{365.25}\right) + \beta_4 \sin\left(4\pi \frac{\text{doy}}{365.25}\right) \quad (9)$$

where T_m^r is the T_m at the grid height, doy is the day of year, and the other coefficients are stored in a regular grid of $1^\circ \times 1^\circ$ and $5^\circ \times 5^\circ$. The realization of the T_m derived from the GPT2w model is accomplished by performing bilinear interpolation for the T_m derived from four surrounding grids of the target position. The code and specific use of the GPT2w model are provided at the website of GGOS Atmosphere (<http://ggosatm.hg.tuwien.ac.at/DELAY/SOURCE/>). The goal of this work is to refine the T_m derived from GPT2w in China, therefore, a sophisticated investigation of spatial–temporal characteristics for the T_m lapse rate is needed.

Investigation of the T_m lapse rate

Height differences between the grid height and the target height have always existed, especially in regions with highly undulating terrain such as western China. Several studies have shown that T_m has a strong correlation with height (Zhang et al. 2017; He et al. 2017). The GPT2w model does not consider the height adjustment for T_m calculation, which results in significant systematic bias for China (Huang et al. 2019). Therefore, it is necessary to perform a height adjustment for the T_m derived from GPT2w model. In this section, we explore the vertical dependence of T_m using gridded T_m

data in 2014 and ellipsoidal height grid data in China. The results are shown in Fig. 2.

Figure 2 shows an approximate linear relationship between T_m and height. The vertical dependence of T_m , therefore, can be expressed as a linear formula:

$$T_m = \gamma \times \delta h + k \tag{10}$$

where γ indicates the T_m lapse rate (K/km) and δh indicates the ellipsoidal height (km).

The T_m lapse rate is undoubtedly a key parameter for the vertical correction of T_m . He et al. (2017) performed an analysis for the global distribution of the T_m lapse rate and showed that the annual mean T_m lapse rate varies with latitude and land–sea distribution across the globe. Nevertheless, relatively smaller variations for the annual mean T_m lapse rate were observed in China, meaning that a uniformed model can be constructed for the vertical correction of T_m in China. Similarly, Zhang et al. (2017) investigation on the four seasons of the T_m lapse rate revealed a seasonal dependence of the T_m lapse rate. However, a sophisticated investigation of seasonal characteristics for the T_m lapse rate is still lacking. In this section, the gridded T_m data from 2007 to 2014 and corresponding ellipsoidal height grid data in China are used to explore the seasonal variations of the T_m lapse rate. In addition, the fast Fourier transform (FFT) algorithm is performed to detect the periodicity characteristics of the T_m lapse rate. The results are shown in Fig. 3.

Figure 3 shows that the T_m lapse rate clearly has seasonal variations. Both annual cycles and semi-annual cycles are detected. The T_m lapse rate, therefore, can be modeled as the following formula:

$$\begin{aligned} \gamma = & \alpha_0 + \alpha_1 \cos\left(2\pi \frac{\text{doy}}{365.25}\right) + \alpha_2 \sin\left(2\pi \frac{\text{doy}}{365.25}\right) \\ & + \alpha_3 \cos\left(4\pi \frac{\text{doy}}{365.25}\right) + \alpha_4 \sin\left(4\pi \frac{\text{doy}}{365.25}\right) \end{aligned} \tag{11}$$

where doym is the day of year; α_0 is the annual mean value of the T_m lapse rate; and (α_1, α_2) and (α_3, α_4) are the coefficients of the annual and semi-annual periodicity of the T_m lapse rate, respectively.

Development of the IGPT2w model in China

The goal of this study is to refine the T_m derived from the GPT2w model and to develop an improved T_m model for China, named IGPT2w. The model formula is as follows:

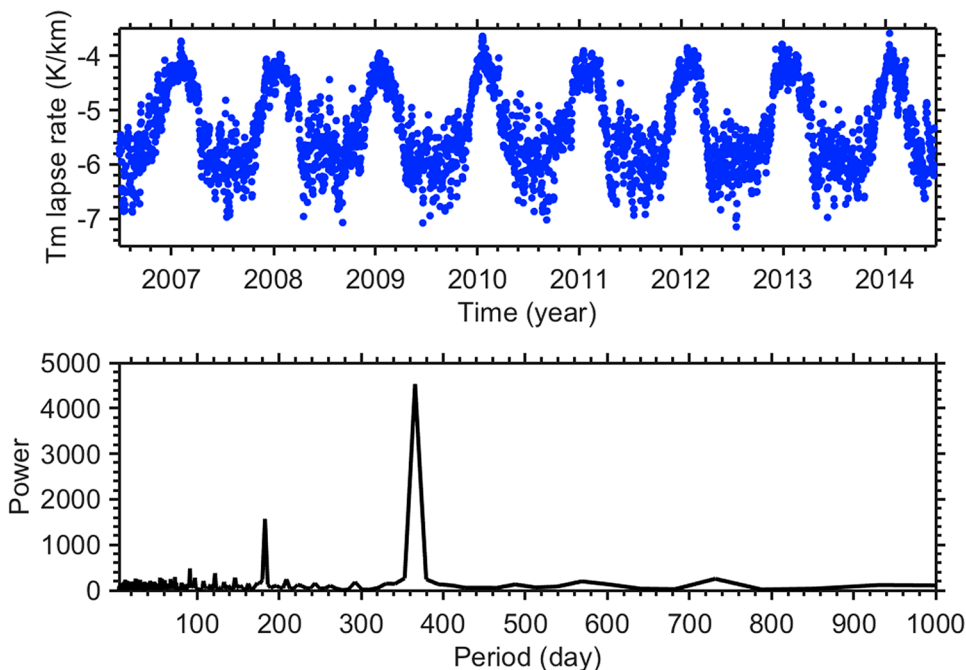
$$T_m^t = T_m^r + \gamma \times (\delta h_t - \delta h_r) \tag{12}$$

where T_m^t is the T_m derived from the IGPT2w model at the target height; T_m^r is the T_m derived from the GPT2w model (9) at the grid height; and δh_t and δh_r are the target height and the grid height in km, respectively. For the T_m lapse rate (γ), which can be estimated by performing the least squares method with gridded T_m data from 2007 to 2014 and

Table 1 Coefficients of the T_m lapse rate model calculated using gridded T_m data from 2007 to 2014 and ellipsoidal gridded height data for China

Coefficients	α_0	α_1	α_2	α_3	α_4
Value	-5.3494	-0.7846	-0.4209	0.1965	0.2680

Fig. 3 Seasonal variations of the T_m lapse rate from 2007 to 2014 in China (top) and results of periodicity detection for the T_m lapse rate using the FFT algorithm (bottom)



ellipsoidal gridded height data for China based on (11), the coefficients of the T_m lapse rate model are shown in Table 1.

Here, a description of the use of the IGPT2w model is provided. There are two steps to realize the T_m derived from the IGPT2w model. First, the vertical correction values of T_m are computed for the four surrounding grids of the target position using the T_m lapse rate model. Next, the T_m at the target height derived from the IGPT2w model is obtained by conducting a bilinear interpolation for the T_m derived from four surrounding grids of the target position. The T_m is derived from the IGPT2w model with the same horizontal resolution as the GPT2w model, i.e., with resolutions of $1^\circ \times 1^\circ$ and $5^\circ \times 5^\circ$.

Validation of IGPT2w

The T_m values derived from the gridded data from the GGOS Atmosphere and the radiosonde data are treated as reference values to evaluate the performance of the IGPT2w model. The results are also compared with the GPT2w model and the Bevis formula ($T_m = 70.2 + 0.72T_s$). As mentioned above, both the IGPT2w and GPT2w models have two horizontal resolutions of $1^\circ \times 1^\circ$ and $5^\circ \times 5^\circ$. For convenience, we defined these two resolutions for each model as IGPT2w-1, IGPT2w-5, GPT2w-1, and GPT2w-5, respectively. In this study, the bias and RMS error are regarded as criteria to assess the accuracy of the models and are calculated using the following formulas:

$$\text{bias} = \frac{1}{N} \sum_{i=1}^N (X_m^{M_i} - X_m^{R_i}) \quad (13)$$

$$\text{RMS} = \sqrt{\frac{1}{N} \sum_{i=1}^N (X_m^{M_i} - X_m^{R_i})^2} \quad (14)$$

where $X_m^{M_i}$ indicates the value calculated by the model, $X_m^{R_i}$ indicates the reference value, and N indicates the number of samples.

Comparison with gridded data from the GGOS Atmosphere

In this experimental area, i.e., the longitude and longitude vary from 70°E to 135°E and 15°N to 55°N , there are a total of 540 T_m grids. The gridded T_m data in 2015 are treated as reference values to evaluate the IGPT2w-1, IGPT2w-5, GPT2w-1, GPT2w-5, and Bevis models. For the Bevis formula ($T_m = 70.2 + 0.72T_s$), since in situ T_s measurements at each grid are unavailable, the T_s value derived from

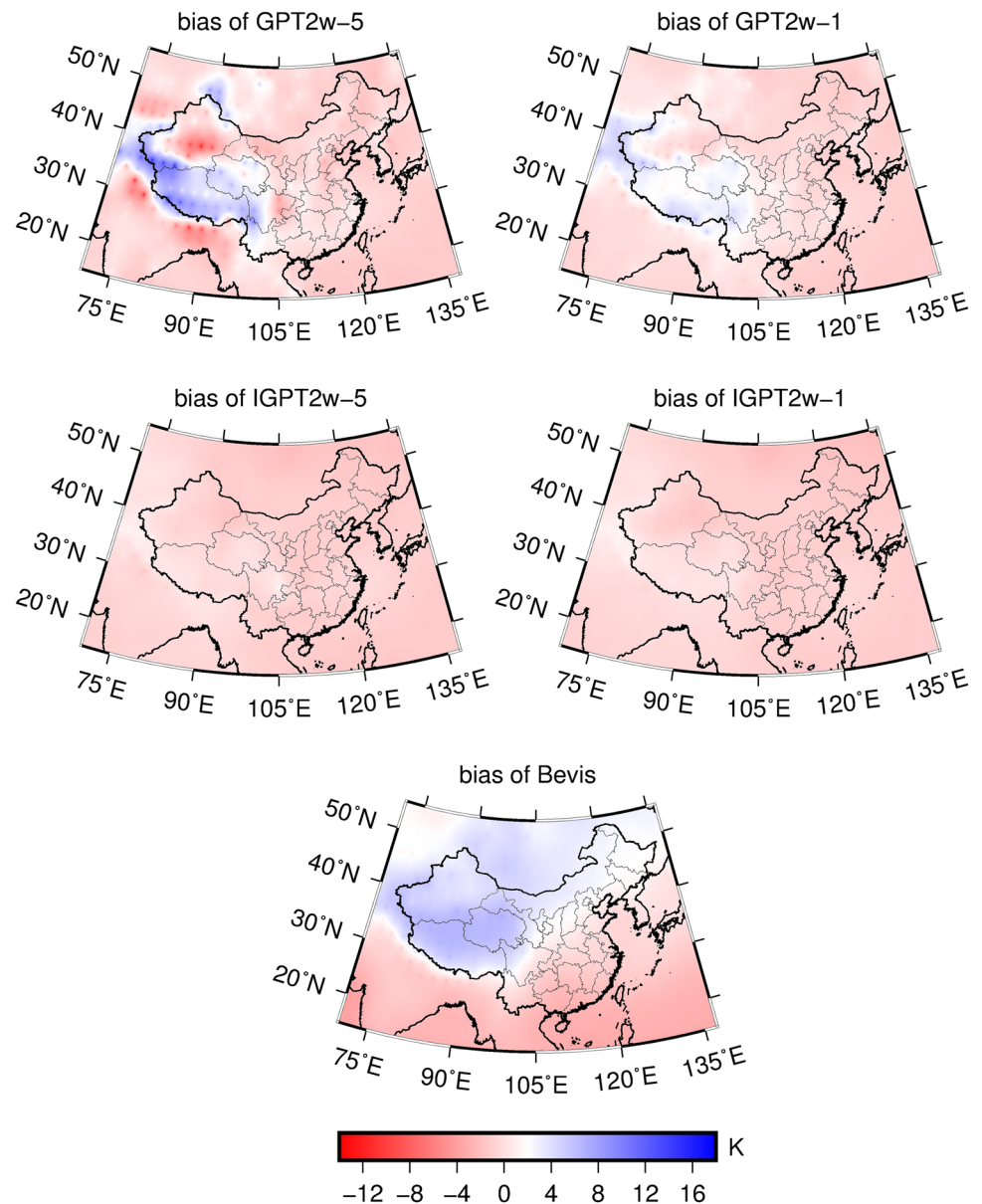
Table 2 Statistical results of different models validated using 2015 gridded T_m data from the GGOS Atmosphere

Model	Bevis	GPT2w-5	GPT2w-1	IGPT2w-5	IGPT2w-1
Bias (in K)					
Max	7.37	17.56	10.30	2.20	1.79
Min	-4.32	-13.52	-2.14	-2.39	-2.39
Mean	1.17	0.19	0.23	-0.78	-0.74
RMS (in K)					
Max	8.38	17.87	10.83	5.32	5.21
Min	1.97	2.10	2.09	1.69	1.70
Mean	4.79	4.50	3.81	3.36	3.32

GPT2w-1 can serve as alternative data for the Bevis formula. Therefore, the statistical results of the annual bias and RMS values of the different models tested by gridded T_m data for 2015 can be obtained and are shown in Table 2 and Figs. 4 and 5.

Table 2 shows that GPT2w-5 and GPT2w-1 have large bias values that range from -13.52 to 17.56 K and -2.14 to 10.30 K, respectively. The Bevis formula has the largest annual mean bias, and both IGPT2w-5 and IGPT2w-1 show stable and small bias values. Similarly, larger RMS values are also obtained for GPT2w-5 and GPT2w-1. The GPT2w-1 has slightly better results than GPT2w-5, while the Bevis formula has the largest annual mean RMS value. In terms of RMS, IGPT2w-5 and IGPT2w-1 have improved by approximately 1.1 K (25%) and 0.5 K (13%) against GPT2w-5 and GPT2w-1, respectively. Thus, the IGPT2w shows significant improvement compared to GPT2w in calculating T_m . Figure 4 shows large warm biases in parts of western China for both GPT2w-5 and GPT2w-1, especially in the Tibetan area for GPT2w-5. The Bevis formula also has large warm biases in parts of northwest China, especially in the Qinghai–Tibetan Plateau, while both IGPT2w-5 and IGPT2w-1 have stable and small biases in China. Figure 5 shows larger RMS in parts of western China for GPT2w-5 and the Bevis formula, especially in the Tibetan, Qinghai, and Xinjiang areas, which are mainly affected by the areas' complex terrain as GPT2w and the Bevis formula do not consider the vertical correction of T_m . GPT2w-1 produces a relatively small RMS compared to GPT2w-5 by improving the spatial resolution of model parameters, but large RMS values still exist in parts of western China. Since the diurnal variations of T_m are ignored in all models, relatively larger RMS values are observed in parts of northeast China, especially for the Bevis formula, where the diurnal variations of T_m are more significant than in other areas (Fig. 6). Nevertheless, the significant errors of the GPT2w and the Bevis formula in high-altitude areas are largely eradicated by the IGPT2w, especially western China. Thus, IGPT2w represents a

Fig. 4 Distribution of bias in different models validated using gridded T_m data for 2015 over China



marked improvement relative to other models in areas with highly undulating terrain. Besides, for IGPT2w, it appears the introduction of the improved altitude correction for T_m reduces the need for a high spatial resolution of the GPT2w model for T_m .

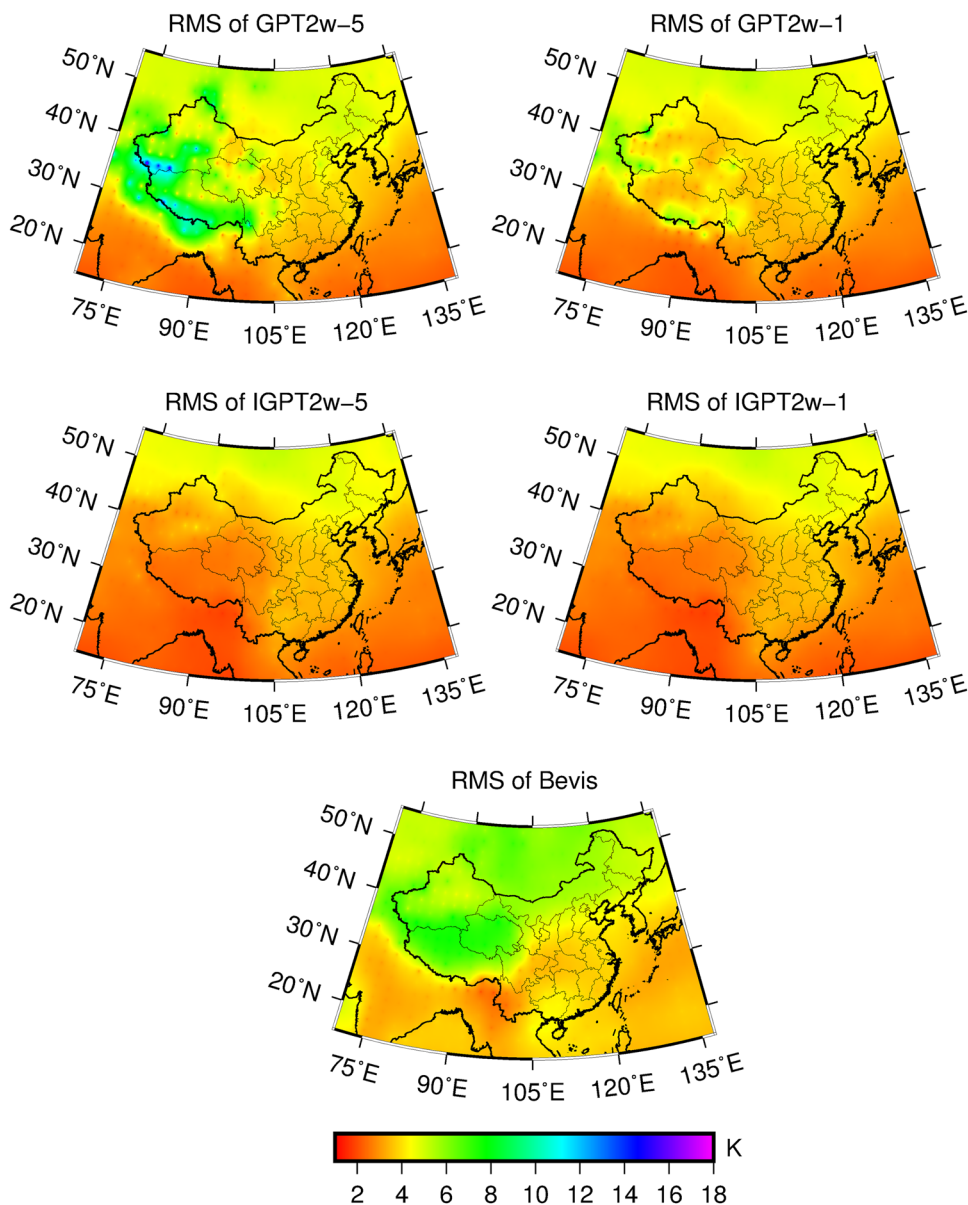
Comparison with radiosonde data

Radiosonde profiles are in situ observations, which are often regarded as the reference values when assessing the performance of other meteorological observing networks or models due to their excellent accuracy and reliability. In this study, a total of 89 radiosonde stations evenly distributed over China are selected (Fig. 1) to validate the performance of IGPT2w and competing T_m models. The T_m values are

calculated from radiosonde profiles stably providing data with 12 h time resolution for half a year. For the Bevis formula, the T_s can also be derived from the radiosonde record. The abnormal radiosonde profiles are removed to ensure the reliability of the assessment. The statistical results of the different models are shown in Table 3 and Figs. 7 and 8.

In Table 3, one can see that GPT2w-5 and GPT2w-1 show larger mean cold bias, which illustrates that GPT2w has a significant systematic bias. The Bevis formula shows a relatively larger mean warm bias, while both IGPT2w-5 and IGPT2w-1 present stable and small biases for China, verifying that the systematic errors of GPT2w are largely eradicated by IGPT2w. In terms of RMS, GPT2w-5 still shows the largest RMS among the models, the Bevis formula has similar performance as GPT2w-1, and IGPT2w-5 and

Fig. 5 Distribution of RMS error in different models validated using gridded T_m data from 2015 in China



IGPT2w-1 show an approximately 0.95 K (20%) and 0.65 K (15%) improvement compared to GPT2w-5 and GPT2w-1, respectively. Clearly the IGPT2w model performs better than other models for China. Figure 7 reflects the larger cold bias in parts of both western China and north of China for GPT2w-5 and GPT2w-1, where significant warm biases are observed for the Bevis formula. In addition, the Bevis formula shows significant cold bias in parts of southeast China, while both IGPT2w-5 and IGPT2w-1 have small and stable biases in all of China. In Fig. 8, one can see that for the Bevis formula the GPT2w-5 and GPT2w-1 still have larger RMS values in parts of western and northern China, especially in Xinjiang province, which is mainly due to the highly undulating terrain and the significant diurnal variations of T_m . For both IGPT2w-5 and IGPT2w-1, those errors are strongly

reduced. The largest remaining errors are observed in parts of northeast China, which are mainly due to not accounting for the diurnal variation of T_m . Overall, both IGPT2w-5 and IGPT2w-1 show stable and excellent performance over China. This further illustrates that IGPT2w shows marked improvement compared to GPT2w in China, especially in areas with strong topographic fluctuations. Additionally, the results of bias and RMS at all radiosonde stations were further analyzed, and the error distribution of the different models are shown in Fig. 9.

From Fig. 9 one can see that GPT2w-5 and GPT2w-1 show larger and significant negative biases. Both have a great proportion of biases below -3 K, and the GPT2w-5 has the largest absolute bias of 13.9 K at the Ruoqiang site, located in Xinjiang province. Although the biases of the

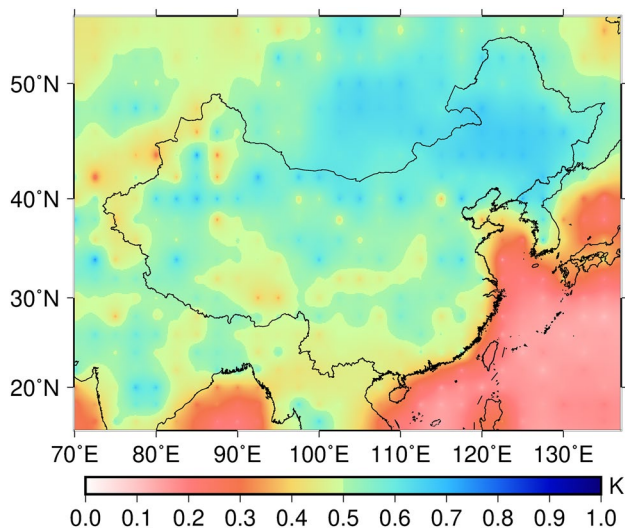


Fig. 6 Distribution of amplitudes of T_m diurnal periodicity across China. The amplitude values of T_m diurnal periodicity are calculated using 2015 gridded T_m data from GGOS Atmosphere

Table 3 Statistical results of different models validated using radiosonde data for 2015

Model	Bevis	GPT2w-5	GPT2w-1	IGPT2w-5	IGPT2w-1
Bias (in K)					
Max	6.81	2.24	1.93	2.62	1.79
Min	-3.55	-13.89	-6.63	-1.80	-1.68
Mean	0.93	-1.67	-1.39	0.02	0.00
RMS (in K)					
Max	7.52	14.42	8.44	5.26	5.35
Min	2.35	2.80	2.54	2.80	2.73
Mean	4.31	4.75	4.43	3.80	3.78

Bevis formula are relatively concentrated around zero, the number of strong negative biases is approximately equal to the number of positive ones, resulting in a relatively small mean bias. The biases of IGPT2w-5 and IGPT2w-1 are small and highly concentrated around zero and are less than 2 K at almost all stations. In terms of RMS, a large proportion of values above 5 K are observed for the Bevis formula, GPT2w-5 and GPT2w-1, while for IGPT2w-5 and IGPT2w-1 the RMS values have a large proportion below 4 K and show high concentration. These results further illustrate that the large errors of GPT2w in estimating T_m are largely removed by IGPT2w.

To analyze the seasonal performance of different models the daily results at all selected stations of each model were statistically analyzed, and the bias and RMS values of different models are varying with the day of year (DOY) are shown in Fig. 10.

In Fig. 10, one can see that both GPT2w-5 and GPT2w-1 show significant cold bias during most DOYs, and larger values are observed during spring and winter days, which further indicates that GPT2w has a significant systematic bias in calculating T_m . The Bevis formula presents a relatively clear warm bias during the spring and a relatively significant cold bias during the summer. Both IGPT2w-5 and IGPT2w-1 show smaller biases without obvious seasonal variation during most DOYs. In terms of RMS, all of these models show relatively clear seasonal variation, with relatively larger RMS values during spring and winter days and smaller ones during summer days. This is because most of the selected radiosonde stations are located in the middle latitudes where T_m changes are small during the summer and larger during the winter. In addition, both GPT2w-5 and GPT2w-1 have larger RMS values than other models at most DOYs. In all, both IGPT2w-5 and IGPT2w-1 have stable and smaller RMS values compared to other models, demonstrating superior seasonal performance.

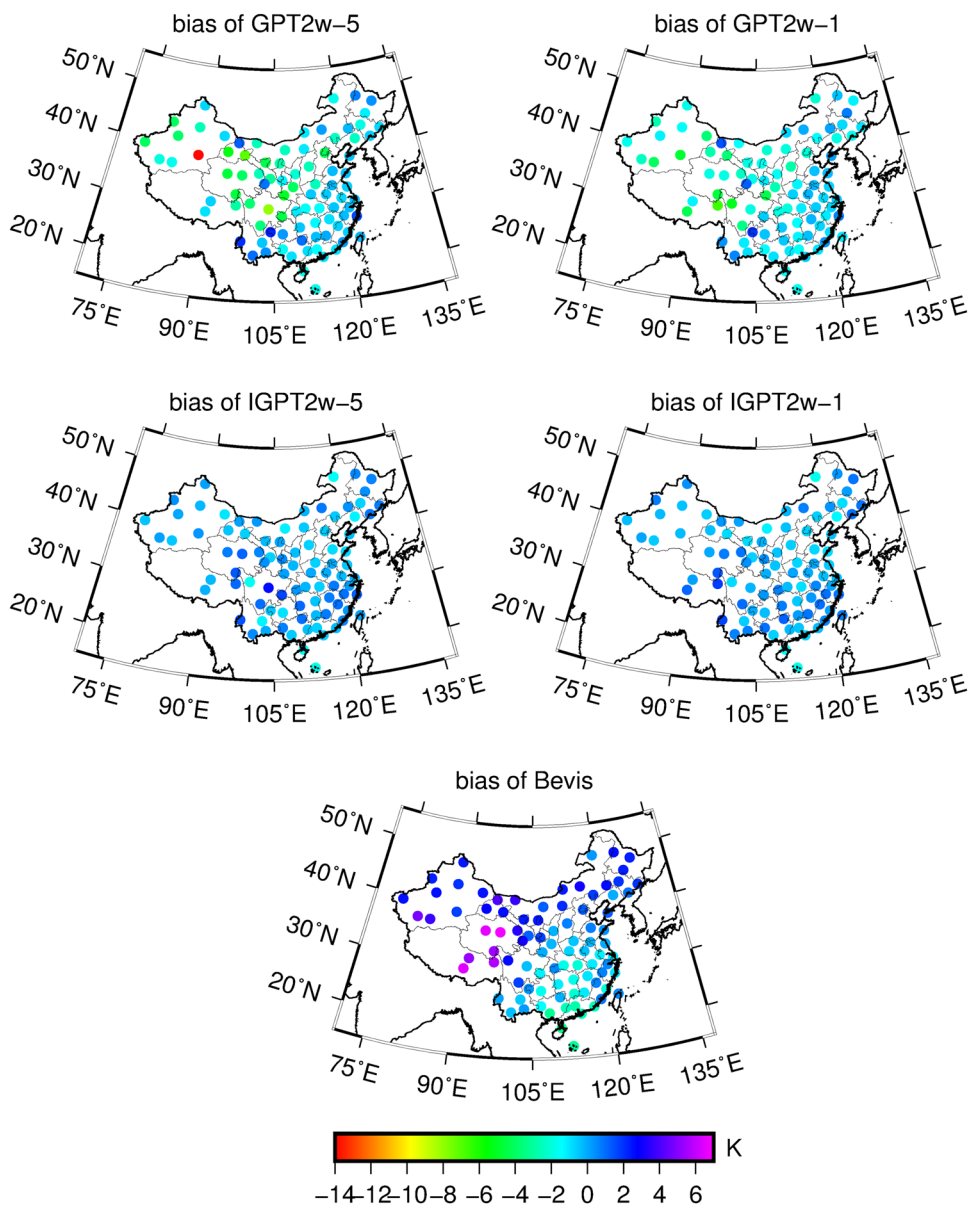
A great number of studies showed that T_m has strong correlations with altitude and latitude (Emardson and Derks 2000; He et al. 2017; Zhang et al. 2017). To investigate how the bias and RMS of different models vary with altitude the 89 selected radiosonde stations were sorted into five groups in terms of altitude, i.e., lower than 500, 500–1000, 1000–1500, 1500–2000, and above 2000 m. The results of the bias and RMS for each altitude range are shown in Fig. 11.

Figure 11 shows that both GPT2w-5 and GPT2w-1 show marked cold bias in all altitude ranges, further indicating that GPT2w has a clear systematic bias in China. The Bevis formula shows larger and significant warm bias in altitudes above 500 m. In general, both bias and RMS of the Bevis formula increase with altitude. In addition, the Bevis formula, GPT2w-5 and the GPT2w-1 present larger RMS values in altitudes above 500 m, which is mainly due to the strongly undulating terrain, while in terms of bias and RMS, IGPT2w-5 and IGPT2w-1 have both stable and excellent performance in all altitude ranges. In all, IGPT2w has superior performance in high-altitude areas compared to other models, although a relative smaller improvement is observed in the altitude range of 1500–2000 m, which is mainly due to the small number of stations located in this altitude range.

Additionally, the relationships between latitude and bias and RMS in different models were also investigated. The 89 selected radiosonde stations were sorted in terms of latitude in 5° intervals. The results are shown in Fig. 12.

From Fig. 12, one can see that both GPT2w-5 and GPT2w-1 still show larger and significant cold biases in all latitude ranges, especially in the areas with a latitude range of 30°–40°. The Bevis formula has a clear warm bias in the latitudes above 35°, while both IGPT2w-5 and IGPT2w-1 show stable and smaller biases in all latitude ranges. The

Fig. 7 Distribution of bias for different models tested using radiosonde data for 2015

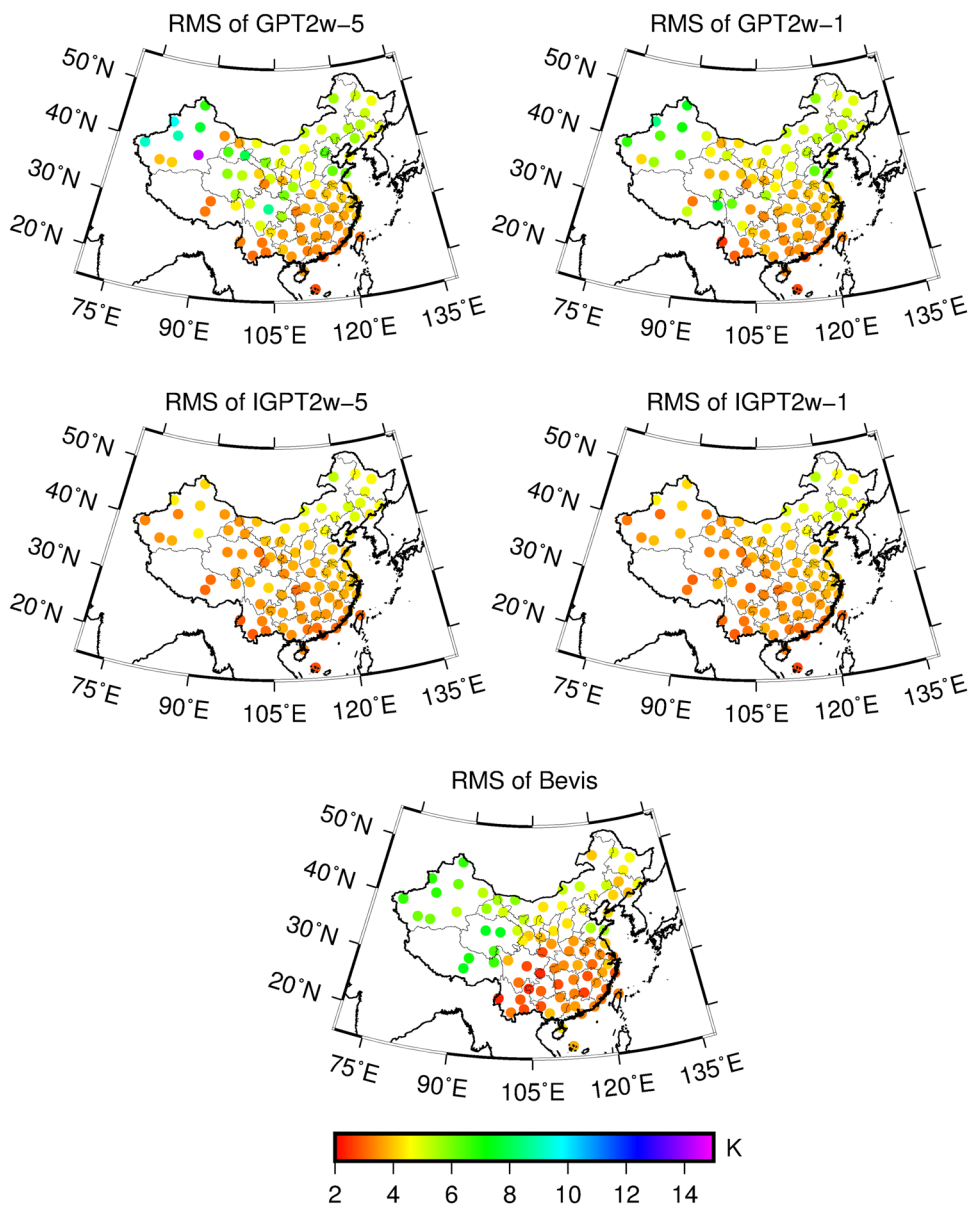


RMS values of all models, in general, increase with increasing latitude in China because the amplitudes of T_m at low latitudes are much smaller than those at high latitudes (Yao et al. 2014b). For all models, relatively larger RMS values are observed in the latitudes above 40°, where the majority stations are located in northeast China, Xinjiang, and Inner Mongolia province, while in these areas the diurnal variations of T_m are more significant than in other areas. Nevertheless, both IGPT2w-5 and IGPT2w-1 still perform significantly superior against other models in the latitudes above 30°.

Impact of T_m on GNSS-PWV

The purpose of estimating T_m is to convert the ZWD into GNSS-PWV. The GNSS stations and radiosonde stations are generally not co-located. In addition, most of the GNSS stations are not equipped with meteorological instruments. Therefore, it is hard to conduct a reliable and comprehensive investigation of the impact of T_m on GNSS-PWV. However, several studies have been conducted to investigate the impact of T_m on its resultant GNSS-PWV in terms of theoretical models (Wang et al. 2005, 2016; Huang et al. 2019). In this work, a similar approach is conducted to investigate the impact of T_m on GNSS-PWV, and the widely used formula of RMS values between T_m and PWV can be written as

Fig. 8 Distribution of RMS for different models tested using radiosonde data for 2015



$$\frac{\sigma_{PWV}}{PWV} = \frac{\sigma_{\Pi}}{\Pi} = \frac{k_3 \sigma_{T_m}}{\left(k'_2 + \frac{k_3}{T_m}\right) T_m^2} = \frac{k_3}{\left(k'_2 + \frac{k_3}{T_m}\right) T_m} \cdot \frac{\sigma_{T_m}}{T_m} \quad (15)$$

where σ_{PWV} is the RMS error of PWV, σ_{T_m} is the RMS error of T_m , T_m and PWV are set to annual mean values, and the σ_{PWV}/PWV is defined as the relative error of PWV. Thus, σ_{PWV} and σ_{PWV}/PWV are employed to assess the impact of the errors in T_m on its resultant GNSS-PWV. In this section, 89 radiosonde stations are also selected throughout China, and the distribution of the theoretical results of σ_{PWV} and σ_{PWV}/PWV is shown in Fig. 13.

Figure 13 shows relatively larger σ_{PWV} values in south-east and south China than other areas for the IGPT2w-5 and

IGPT2w-1 models, and the PWV values are larger than in other areas because PWV values play a dominant role in σ_{PWV} calculation. The σ_{PWV} values of the IGPT2w model are less than 0.59 mm and with a mean σ_{PWV} value of 0.29 mm. In terms of σ_{PWV}/PWV , the IGPT2w has a mean value of 1.38% and ranges from 0.95 to 2.0%, which is more stable and smaller than when using T_m from the other models under study. The IGPT2w is an empirical model, which can provide an accurate T_m for retrieving accurate real-time PWV values. Therefore, IGPT2w has possible potential applications in nowcasting or real-time analysis of severe weather conditions, such as heavy rainfall, typhoons, and flood forecasting in China, and also can be used to retrieve high-precision GNSS-PWV values for the study of PWV transportation in the Tibetan plateau.

Fig. 9 Histogram of bias and RMS for different models tested using radiosonde data for 2015

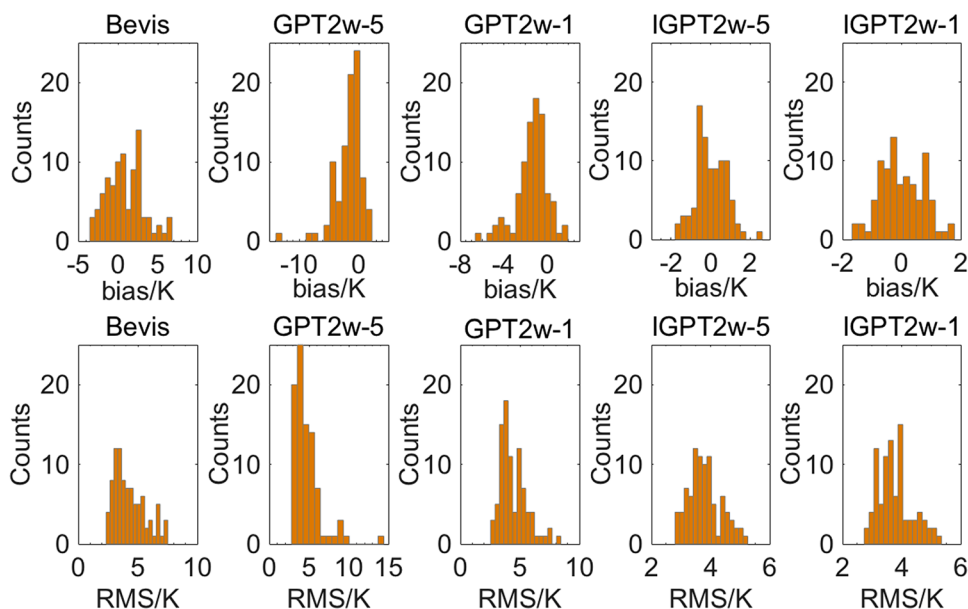
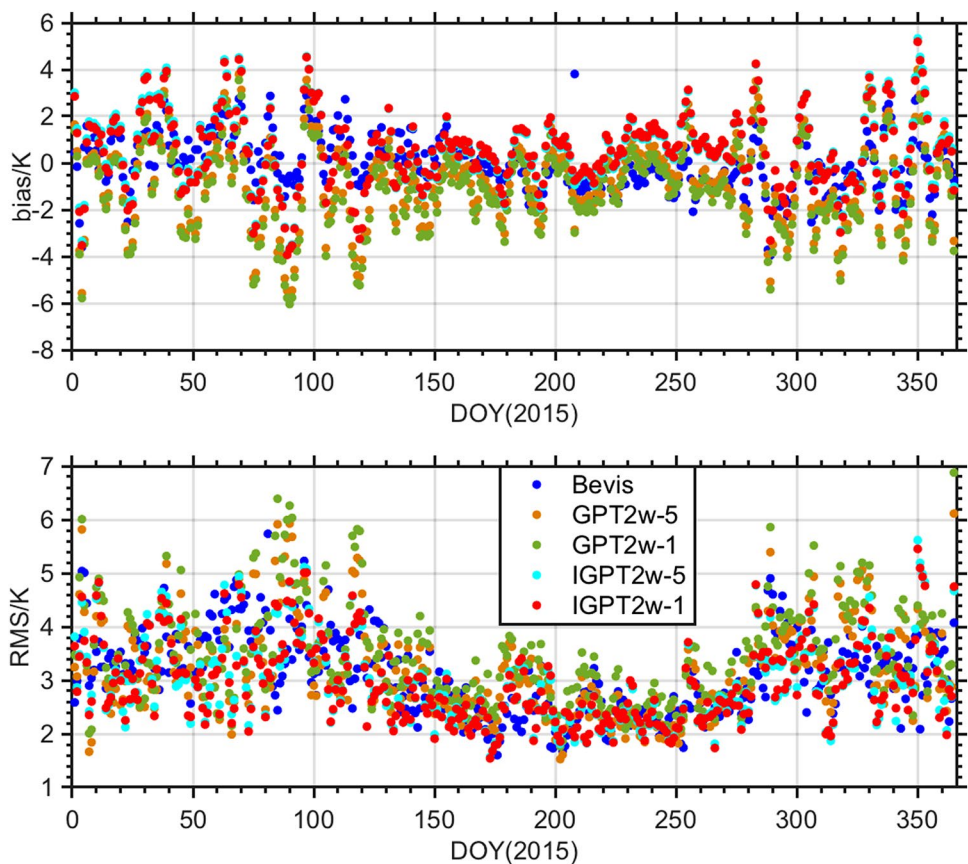


Fig. 10 Results of different models validated using radiosonde data during different days of the year



Conclusions

T_m plays an important role in the process of retrieving PWV values from GNSS signals. In real-time GNSS-PWV sounding in China, an accurate and reliable empirical T_m model

is needed. The GPT2w is one of the state-of-the-art tropospheric models, which has excellent performance compared to existing empirical models for T_m calculation. However, the GPT2w has a systematic error in T_m estimation for China because the vertical correction of T_m is ignored. We

Fig. 11 Results of bias and RMS of the different models at different altitude ranges

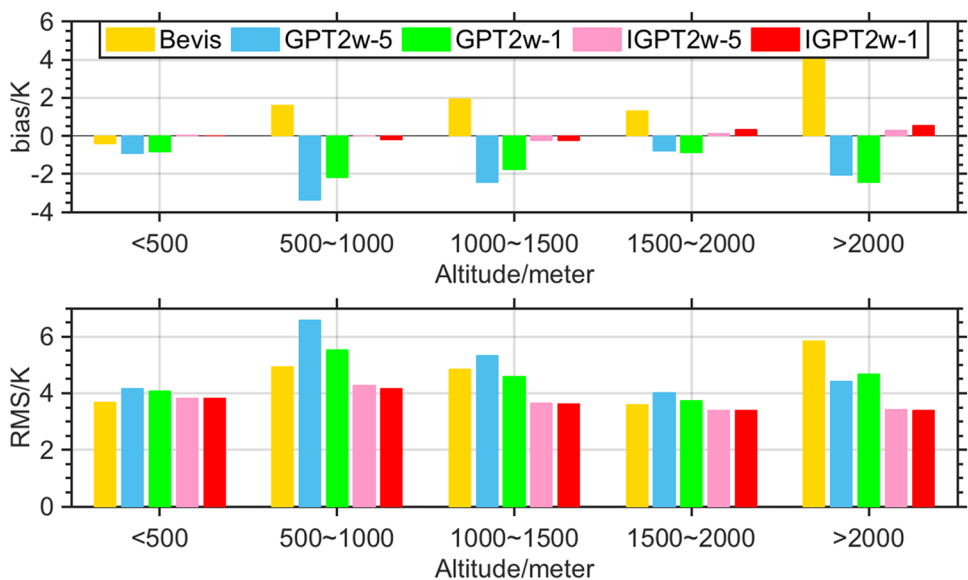
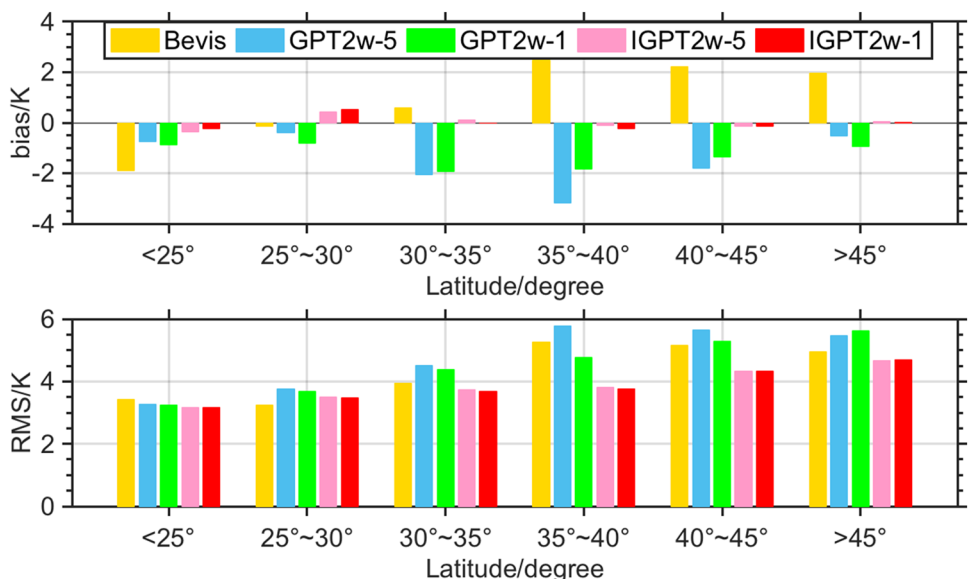


Fig. 12 Results of bias and RMS of the different models at different latitude ranges



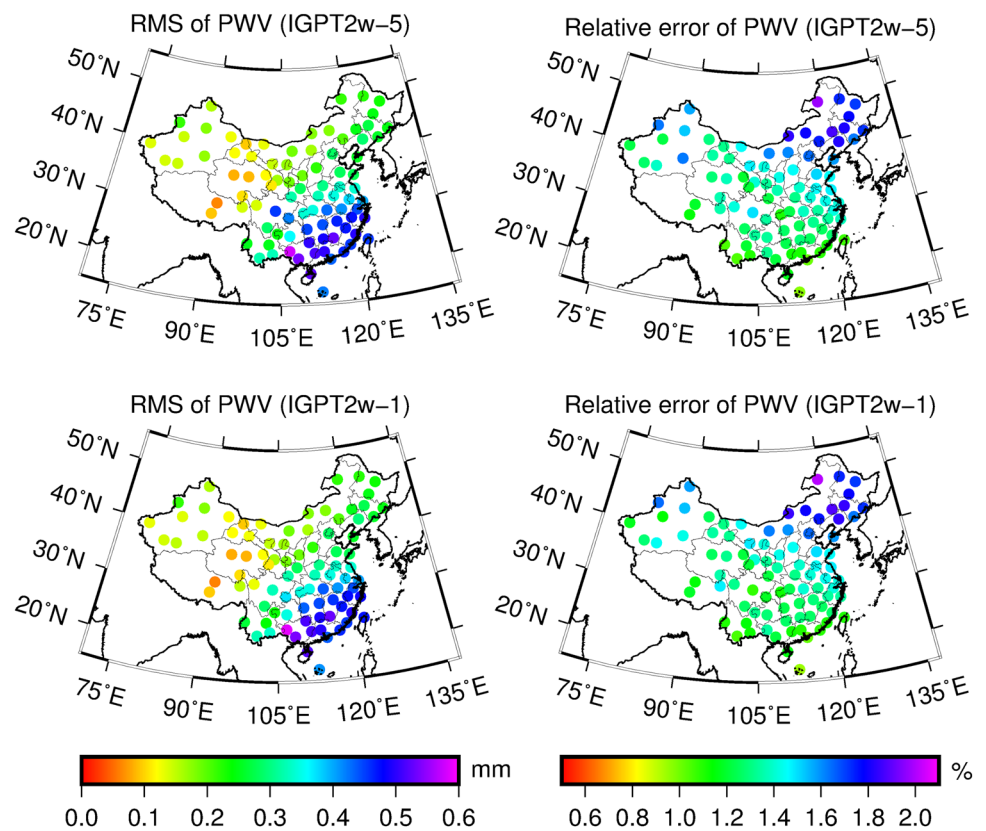
considered the vertical adjustment of T_m in modeling, and the T_m lapse rate model was developed for China using ellipsoidal height grid data and gridded T_m data from the GGOS Atmosphere. Finally, an improved atmospheric weighted mean temperature model, IGPT2w, was developed by refining the T_m derived from GPT2w in China.

The performance of IGPT2w was tested using both gridded T_m data and radiosonde site records in 2015 over China, and comprehensive comparisons to GPT2w and the Bevis formula were also performed. The results show a strong performance enhancement of the IGPT2w model against other models for China, especially in western China, where larger errors of the GPT2w model were largely removed. The impact of T_m derived from IGPT2w on GNSS-PWV was also investigated, showing that the mean values of σ_{PWV} and

σ_{PWV}/PWV are 0.29 mm and 1.38% for IGPT2w in terms of GNSS-PWV retrieval, respectively.

In this work, the GPT2w had significant systematic errors in western China, and poorer results were achieved for the Bevis formula in both northwest and north China. IGPT2w had significant improvements compared to GPT2w in T_m estimation over China, especially in western China. IGPT2w is an empirical model and has the ability to provide reliable and accurate T_m values for China, making it more powerful for estimating real-time T_m values and giving it wide potential in real-time GNSS-PWV sounding, especially for application in western China. In future work, we will focus on accounting for diurnal variation of T_m in the model and will improve the estimation of T_m from GPT2w on a global scale.

Fig. 13 Theoretical RMS error and relative error of PWV resulting from the IGPT2w model using radiosonde data for 2015



Acknowledgements This work was sponsored by the National Natural Foundation of China (41704027; 41664002); the National Science Foundation for Distinguished Young Scholars of China (41525014); Guangxi Natural Science Foundation of China (2017GXNS-FBA198139; 2017GXNSFDA198016); the Major Project of Beijing Future Urban Design Innovation Center, Beijing University of Civil Engineering and Architecture (UDC 2018031321); the “Ba Gui Scholars” program of the provincial government of Guangxi; and the Guangxi Key Laboratory of Spatial Information and Geomatics (16-380-25-01; 15-140-07-19). The authors would like to thank the GGOS Atmosphere for providing gridded data and the University of Wyoming for providing radiosonde profiles.

References

- Adams DK, Gutman SI, Holub KL, Pereira DS (2013) GNSS observations of deep convective time scales in the Amazon. *Geophys Res Lett* 40:2818–2823
- Askne J, Nordius H (1987) Estimation of tropospheric delay for microwaves from surface weather data. *Radio Sci* 22:379–386
- Benevide P, Catalao J, Miranda PMA (2015) On the inclusion of GPS precipitable water vapour in the nowcasting of rainfall. *Nat Hazards Earth Syst Sci* 15(12):2605–2616
- Bevis M, Businger S, Chiswell S, Herring TA, Rocken C, Anthes RA, Ware RH (1992) GPS meteorology: remote sensing of atmospheric water vapor using the global positioning system. *J Geophys Res* 97(D14):15787–15801
- Bevis M, Businger S, Chiswell S, Herring TA, Anthes RA, Rocken C, Ware RH (1994) GPS meteorology: mapping zenith wet delays onto precipitable. *J Appl Meteorol* 33:379–386
- Böhm J, Heinkelmann R, Schuh H (2007) Short note: a global model of pressure and temperature for geodetic applications. *J Geod* 81(10):679–683
- Böhm J, Moller G, Schindelegger M, Pain G, Weber R (2015) Development of an improved empirical model for slant delays in the troposphere (GPT2w). *GPS Solut* 19(3):433–441
- Bolton D (1980) The computation of equivalent potential temperature. *Mon Weather Rev* 108:1046–1053
- Byun SH, Bar-Sever YE (2009) A new type of troposphere zenith path delay product of the international GNSS service. *J Geod* 83(3–4):1–7
- Chen P, Yao WQ, Zhu XJ (2014) Realization of global empirical model for mapping zenith wet delays onto precipitable water using NCEP re-analysis data. *Geophys J Int* 198:1748–1757
- Davis JL, Herring TA, Shapiro II, Rogers AEE, Elgered G (1985) Geodesy by radio interferometry: effects of atmospheric modeling errors on estimates of baseline length. *Radio Sci* 20:1593–1607
- Ding MH (2018) A neural network model for predicting weighted mean temperature. *J Geod* 92(10):1187–1198
- Emardson TR, Derks HJP (2000) On the relation between the wet delay and the integrated precipitable water vapour in the European atmosphere. *Meteorol Appl* 7:61–68
- He CY, Wu SQ, Wang XM, Hu AD, Wang QX, Zhang KF (2017) A new voxel-based model for the determination of atmospheric weighted mean temperature in GPS atmospheric sounding. *Atmos Meas Tech* 10(6):2045–2060
- Hobiger T, Ichikawa R, Takasu T, Koyama Y, Kondo T (2008a) Ray-traced troposphere slant delays for precise point positioning. *Earth Planets Space* 60(5):e1–e4
- Hobiger T, Ichikawa R, Koyama Y, Kondo T (2008b) Fast and accurate ray-tracing algorithms for real-time space geodetic applications

- using numerical weather models. *J Geophys Res* 113:D20302. <https://doi.org/10.1029/2008JD010503>
- Huang LK, Jiang WP, Liu LL, Chen H, Ye SR (2019) A new global grid model for the determination of atmospheric weighted mean temperature in GPS precipitable water vapor. *J Geod* 93(2):159–176
- Huelsing HK, Wang JH, Mears C, Braun JJ (2017) Precipitable water characteristics during the 2013 Colorado flood using ground-based GPS measurements. *Atmos Meas Tech* 10:4055–4066
- Jiang WP, Yuan P, Chen H, Cai JQ, Li Z, Chao NF, Sneeuw N (2017) Annual variations of monsoon and drought detected by GPS: a case study in Yunnan, China. *Sci Rep* 7:5874
- Jin SG, Luo OF (2009) Variability and climatology of PWV from global 13-year GPS observations. *IEEE T Geosci Remote Sens* 47(7):1918–1924
- Li XX, Dick G, Lu CX, Ge MR, Nilsson T, Ning T, Wickert J, Schuh H (2015) Multi-GNSS meteorology: real-time retrieving of atmospheric water vapor from BeiDou, Galileo, GLONASS, and GPS observations. *IEEE Trans Geosci Remote Sens* 53(12):6385–6393
- Lu CX, Zus F, Ge MR, Heinkelmann R, Dick G, Wickert J, Schuh H (2016) Tropospheric delay parameters from numerical weather models for multi-GNSS precise positioning. *Atmos Meas Tech* 9(12):5965–5973
- Lu CX, Li XX, Zus F, Heinkelmann R, Dick G, Ge MR, Wickert J, Schuh H (2017) Improving BeiDou real-time precise point positioning with numerical weather models. *J Geod* 91(9):1019–1029
- Manandhar S, Lee Y, Meng Y, Ong J (2017) A simplified model for the retrieval of precipitable water vapor from GPS signal. *IEEE Trans Geosci Remote Sens* 55(11):6245–6253
- Rocken C, Hove TV, Johnson J, Solheim F, Ware R, Bevis M, Chiswell S, Businger S (1995) GPS/STORM-GPS sensing of atmospheric water vapor for meteorology. *J Atmos Oceanic Technol* 12(3):468–478
- Ross RJ, Rosenfeld S (1997) Estimating mean weighted temperature of the atmosphere for Global Positioning System applications. *J Geophys Res Atmos* 102:21719–21730
- Suparta W, Rahman R (2016) Spatial interpolation of GPS PWV and meteorological variables over the west coast of Peninsular Malaysia during 2013 Klang Valley Flash Flood. *Atmos Res* 168:205–219
- Wang JH, Zhang LY (2009) Climate applications of a global, 2-hourly atmospheric precipitable water dataset derived from IGS tropospheric products. *J Geod* 83(3–4):209–217
- Wang JH, Zhang LY, Dai AG (2005) Global estimates of water-vapor-weighted mean temperature of the atmosphere for GPS applications. *J Geophys Res*. <https://doi.org/10.1029/2005JD006215>
- Wang JH, Zhang LY, Dai AG, Van Hove T, Van Baelen J (2007) A near-global, 2-hourly data set of atmospheric precipitable water from ground-based GPS measurements. *J Geophys Res Atmos*. <https://doi.org/10.1029/2006JD007529>
- Wang XM, Zhang KF, Wu SQ, Fan SJ, Cheng YY (2016) Water vapor-weighted mean temperature and its impact on the determination of precipitable water vapor and its linear trend. *J Geophys Res Atmos* 121:833–852
- Yao Y, Zhu S, Yue S (2012) A globally applicable, season-specific model for estimating the weighted mean temperature of the atmosphere. *J Geod* 86(12):1125–1135
- Yao YB, Zhang B, Yue SQ, Xu CQ, Peng WF (2013) Global empirical model for mapping zenith delays onto precipitable. *J Geod* 87(5):439–448
- Yao YB, Zhang B, Xu CQ, Yan F (2014a) Improved one/multiparameter models that consider seasonal and geographic variations for estimating weighted mean temperature in ground-based GPS meteorology. *J Geod* 88(3):273–282
- Yao YB, Xu CQ, Zhang B, Cao N (2014b) GTm-III: a new global empirical model for mapping zenith wet delays onto precipitable water vapor. *Geophys J Int* 197:202–212
- Yao CL, Luo ZC, Liu LL, Zhou BY (2015) On the relation between the wet delay and the precipitable water vapor in consideration of topographic relief in the low-latitude region of China. *Geomat Inf Sci Wuhan Univ* 40(7):907–912
- Zhang K, Manning T, Wu S, Rohm W, Silcock D, Choy S (2015) Capturing the signature of severe weather events in Australia using GPS measurements. *IEEE J Sel Top Appl Earth Obs Remote Sens* 8(4):1839–1847
- Zhang HX, Yuan YB, Li W, Ou JK, Li Y, Zhang BC (2017) GPS PPP-derived precipitable water vapor retrieval based on T_m/P_s from multiple sources of meteorological data sets in China. *J Geophys Res Atmos*. <https://doi.org/10.1002/2016JD026000>
- Zhao QZ, Yao YB, Yao WQ (2018) GPS-based PWV for precipitation forecasting and its application to a typhoon event. *J Atmos Sol Terr Phys* 167:124–133

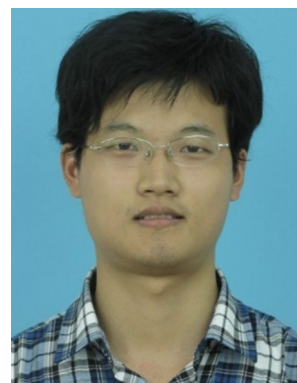
Publisher's Note Springer Nature remains neutral with regard to jurisdictional claims in published maps and institutional affiliations.



Liangke Huang is a Ph.D. candidate at the GNSS Research Center, Wuhan University. He received his B.Sc. degree in 2011 from Guilin University of Technology. His current research mainly focuses on GNSS meteorology and tropospheric modeling.



Lilong Liu is currently a professor at the Guilin University of Technology. He obtained his Ph.D. degree in Geodesy and Engineering Surveying at the School of Geodesy and Geomatics in Wuhan University in 2005. His main research interests include GNSS data processing, GNSS ionospheric monitoring, and GNSS atmospheric modeling.



Hua Chen is currently a postdoctor at Wuhan University. He obtained his B.Sc., Master and Ph.D. degrees with distinction in Geodesy and Engineering Surveying at the School of Geodesy and Geomatics in Wuhan University in 2009, 2011 and 2015. His main research interests include GNSS data processing of large-scale networks, GNSS orbit determination, and atmospheric parameter estimation.



Weiping Jiang is currently a professor at the Wuhan University. He obtained his B.Sc., Master and Ph.D. degrees with distinction in Geodesy and Engineering Surveying at the School of Geodesy and Geomatics in Wuhan University in 1995, 1997

and 2001. His main research interests include GNSS data processing of large-scale networks, GNSS space environment, satellite altimetry and geodynamics research.